Distributed gain in plasmonic reflectors and its use for terahertz generation

O. Sydoruk,* R. R. A. Syms, and L. Solymar

Optical and Semiconductor Devices Group, Department of Electrical and Electronic Engineering, Imperial College London, Exhibition Road, London SW7 2AZ, UK

**osydoruk@imperial.ac.uk*

Abstract: Semiconductor plasmons have potential for terahertz generation. Because practical device formats may be quasi-optical, we studied theoretically distributed plasmonic reflectors that comprise multiple interfaces between cascaded two-dimensional electron channels. Employing a mode-matching technique, we show that transmission through and reflection from a single interface depend on the magnitude and direction of a dc current flowing in the channels. As a result, plasmons can be amplified at an interface, and the cumulative effect of multiple interfaces increases the total gain, leading to plasmonic reflection coefficients exceeding unity. Reversing the current direction in a distributed reflector, however, has the opposite effect of plasmonic deamplification. Consequently, we propose structurally asymmetric resonators comprising two different distributed reflectors and predict that they are capable of terahertz oscillations at low threshold currents.

OCIS codes: (260.3090) Infrared, far; (240.6680) Surface plasmons; (230.4910) Oscillators.

References and links

1. J. Gómez Rivas, M. Kuttge, P. H. Bolivar, H. Kurz, and J. A. Sánchez-Gil, "Propagation of surface plasmon polaritons on semiconductor gratings," Phys. Rev. Lett. **93**, 256804 (2004).
2. D. Veksler, F. Teppe, A. P. Dmitriev, V. Y. Kachorovskii, W. Knap, and M. S. Shur, "Detection of terahertz radiation in gated two-dimensional structures governed by dc current," Phys. Rev. B **73**, 125328 (2006).
3. E. Hendry, F. J. Garcia-Vidal, L. Martin-Moreno, J. Gómez Rivas, M. Bonn, A. P. Hibbins, and M. J. Lockyear, "Optical control over surface-plasmon-polariton-assisted THz transmission through a slit aperture," Phys. Rev. Lett. **100**, 123901 (2008).
4. S. A. Mikhailov, "Plasma instability and amplification of electromagnetic waves in low-dimensional electron systems," Phys. Rev. B **58**, 1517–1532 (1998).
5. S. Riyopoulos, "THz instability by streaming carriers in high mobility solid-state plasmas," Phys. Plasmas **12**, 070704 (2005).
6. S. M. Kukhtaruk, "High-frequency properties of systems with drifting electrons and polar optical phonons," Sem. Phys. Quant. Electr. & Optoelectr. **11**, 43–49 (2008).
7. O. Sydoruk, V. Kalinin, and L. Solymar, "Terahertz instability of optical phonons interacting with plasmons in two-dimensional electron channels," Appl. Phys. Lett. **97**, 062107 (2010).
8. M. Dyakonov and M. Shur, "Shallow water analogy for a ballistic field-effect transistor: new mechanism of plasma wave generation by a dc current," Phys. Rev. Lett. **71**, 2465–2468 (1993).
9. F. J. Crowne, "Contact boundary conditions and the Dyakonov–Shur instability in high electron mobility transistors," J. Appl. Phys. **82**, 1242–1254 (1997).
10. M. V. Cheremisin and G. G. Samsonidze, "D'yakonov–Shur instability in a ballistic field-effect transistor with a spatially nonuniform channel," Semiconductors **33**, 578–585 (1999).
11. M. Dyakonov and M. Shur, "Current instability and plasma waves generation in ungated two-dimensional electron layers," Appl. Phys. Lett. **87**(11), 111501 (2005).

#169158 - $15.00 USD Received 23 May 2012; revised 29 Jun 2012; accepted 2 Jul 2012; published 13 Aug 2012

12. O. Sydoruk, R. R. A. Syms, and L. Solymar, "Plasma oscillations and terahertz instability in field-effect transistors with Corbino geometry," Appl. Phys. Lett. **97**, 263504 (2010).
13. J. Lusakowski, W. Knap, N. Dyakonova, L. Varani, J. Mateos, T. Gonzalez, Y. Roelens, S. Bollaert, A. Cappy, and K. Karpierz, "Voltage tuneable terahertz emission from a ballistic nanometer InGaAs/InAlAs transistor," J. Appl. Phys. **97**, 064307 (2005).
14. Y. Tsuda, T. Komori, A. El Fatimy, K. Horiike, T. Suemitsu, and T. Otsuji, "Application of plasmon-resonant microchip emitters to broadband terahertz spectroscopic measurement," J. Opt. Soc. Am. B **26**, A52–A57 (2009).
15. A. El Fatimy, N. Dyakonova, Y. Meziani, T. Otsuji, W. Knap, S. Vandenbrouk, K. Madjour, D. Theron, C. Gaquiere, M. A. Poisson, S. Delage, P. Prystawko, and C. Skierbiszewski, "AlGaN/GaN high electron mobility transistors as a voltage-tunable room temperature terahertz sources," J. Appl. Phys. **107**, 024504 (2010).
16. T. Otsuji, T. Watanabe, A. El Moutaouakil, H. Karasawa, T. Komori, A. Satou, T. Suemitsu, M. Suemitsu, E. Sano, W. Knap, and V. Ryzhii, "Emission of terahertz radiation from two-dimensional electron systems in semiconductor nano- and hetero-structures," J. Infrared Milli. Terahz. Waves **32**, 629—645 (2011).
17. R. E. Collin, *Foundations for Microwave Engineering* (Wiley-IEEE Press, Hoboken, New Jersey, 2001).
18. A. D. Bresler, G. H. Joshi, and N. Marcuvitz, "Orthogonality properties for modes in passive and active uniform wave guides," J. Appl. Phys. **29**, 794–799 (1958).
19. R. F. Oulton, D. F. P. Pile, Y. Liu, and X. Zhang, "Scattering of surface plasmon polaritons at abrupt surface interfaces: Implications for nanoscale cavities," Phys. Rev. B **76**, 035,408 (2007).
20. S. Thongrattanasiri, J. Elser, and V. A. Podolskiy, "Quasi-planar optics: computing light propagation and scattering in planar waveguide arrays," J. Opt. Soc. Am. B **26**, B102–B110 (2009).
21. U. Mackens, D. Heitmann, L. Prager, J. P. Kotthaus, and W. Beinvogl, "Minigaps in the plasmon dispersion of a two-dimensional electron gas with spatially modulated charge density," Phys. Rev. Lett. **53**, 1485–1488 (1984).
22. Z. Knittl, *Optics of Thin Films* (Wiley, London, 1981).

1. Introduction

There has been increased interest in semiconductor plasmons [1–3] due to the rapid development of terahertz science and technology, the most exciting prospect being the realization of oscillators. Various generation mechanisms have been considered theoretically, including, for example, plasmon interactions with quantum-wire gratings [4] or optical phonons [5–7], and the Dyakonov-Shur instability [8]. The latter has inspired a number of theoretical [9–12] and experimental [13–15] studies, but the terahertz power attainable was low (see Ref. [16] for a review). Nevertheless, the lack of cheap and effective terahertz sources continues to motivate further intensive search of plasmonic mechanisms.

Here, we propose quasi-optical terahertz oscillators that are based on distributed reflectors comprising two-dimensional channels with different electron densities (see Fig. 1(a)). In stark contrast to traditional Bragg lasers, the reflectors in our devices are responsible for both the feedback and the gain. The gain occurs at an interface between two channels in the presence of a dc current. Combining interfaces into a periodic superlattice increases the gain, resulting in plasmonic reflection coefficients in excess of unity. Resonators formed by such reflectors are able to oscillate in the terahertz range.

We describe the distributed plasmonic gain in three steps. Section 2, first, discusses a single two-dimensional channel in the presence of dc current and emphasises its non-reciprocal properties. Then, it discusses interfaces between two channels and demonstrates amplification. Section 3 discusses distributed reflectors and shows how these can form oscillators. Section 4 draws conclusions.

2. Single plasmonic reflectors

Consider first an infinitely long electron channel with a dc electron density n_0 surrounded by a dielectric with a relative permittivity ε_d and sandwiched between two perfectly conducting planes placed symmetrically at a distance w from the channel. The geometry is as shown in Fig. 1(a) but with a single homogenous channel instead of a set of cascaded sections. The role of the metallic boundaries is to control the mode spectrum. We assumed TM waves with electric field components E_x and E_z, magnetic field component H_y, angular frequency ω, and

#169158 - $15.00 USD Received 23 May 2012; revised 29 Jun 2012; accepted 2 Jul 2012; published 13 Aug 2012

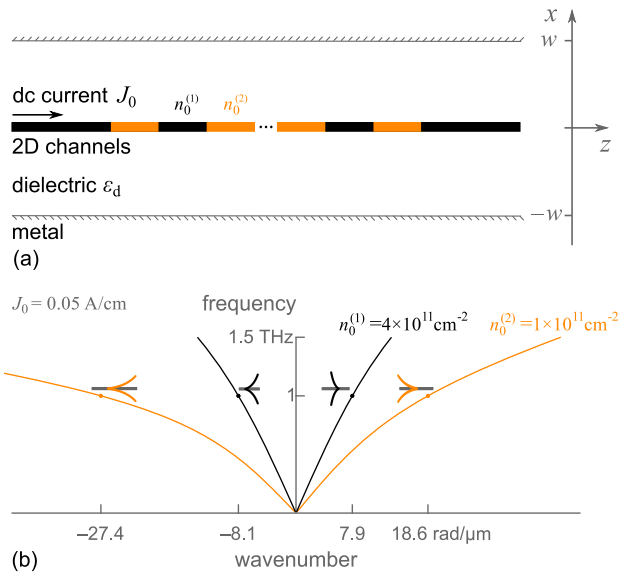

Fig. 1. Cascaded two-dimensional channels form a distributed reflector (a). In the presence of dc current, counter-propagating plasmons have different dispersion characteristics (b) leading to different transverse field profiles, shown schematically on the dispersion curves.

wavenumbers k_x and k_z. The relationship between the wavenumbers is $k_x^2 + k_z^2 = \varepsilon_d \omega^2/c^2$, where c is the light velocity. The boundary conditions are $E_z|_{x=\pm w} = 0$ at the metal and

$$\begin{aligned} E_z|_{x=+0} &= E_z|_{x=-0} \\ E_x|_{x=+0} - E_x|_{x=-0} &= en/(\varepsilon_0 \varepsilon_d) \\ H_y|_{x=+0} - H_y|_{x=-0} &= J \end{aligned} \tag{1}$$

at the channel. Here e is the electron charge; ε_0 is the vacuum permittivity; n and J are, respectively, the harmonically varying electron and current densities. Solution of Maxwell's equations in the dielectric yields the field components; for example, the amplitude of the magnetic field above the channel is

$$H_y = A \frac{\cos k_x (x - w)}{\cos k_x w}, \tag{2}$$

where A is a constant.

We described the electron dynamics using the standard linearized hydrodynamic model [4–12] as follows. The total electron density, n_{tot}, and velocity, v_{tot}, have the form

$$\begin{aligned} n_{tot} &= n_0 + n \\ v_{tot} &= v_0 + v \end{aligned} \tag{3}$$

where v_0 and v are the dc and the ac electron velocities, respectively. As is usually done, we then assumed that the amplitudes of the dc components are much smaller than their dc counterparts and ignored the products of the small quantities $n \times v$ and $v \times v$. Hence, for the total current density we had

$$J_{tot} = e(n_0 + n)(v_0 + v) \approx en_0 v_0 + en_0 v + env_0, \tag{4}$$

The first term of the right-hand side in Eq. (4) is the dc component of the total current density, $J_0 = en_0 v_0$, and the sum of the last two terms is the ac component of the total current density,

#169158 - $15.00 USD Received 23 May 2012; revised 29 Jun 2012; accepted 2 Jul 2012; published 13 Aug 2012

$J = en_0 v + env_0$. Note that the dc current density is independent of the ac components, but the ac current density is affected by the dc components. The latter indicates coupling between the plasmons and drifting electrons, which is responsible for the plasmonic gain discussed below. If the amplitudes of the ac and dc components of the electron density and velocity have comparable values, the term $n \times v$ in Eq. (4) can no longer be neglected. It would, in particular, lead to a dc current due to the ac fields. We were, however, concerned with the onset of oscillations when the ac terms are small and Eq. (4) is valid.

Under the above assumptions, the linearized lossless equation of motion has the form

$$\mathrm{j}(\omega - k_z v_0)v = \frac{e}{m} E_z|_{x=0}\,, \tag{5}$$

where j is the imaginary unit, and m is the electron effective mass. Substituting Eqs. (2), (4), and (5) into Eq. (1) leads to the dispersion relation in the form

$$\Omega_\mathrm{p}^2 \frac{k_x \tan k_x w}{(\omega - k_z v_0)^2} = -1\,, \tag{6}$$

where $\Omega_\mathrm{p}^2 = e^2 n_0/(2m\varepsilon_0\varepsilon_\mathrm{d})$. The dispersion relation's salient feature is its dependence on the electron drift velocity v_0. Due to the Doppler term $k_z v_0$, waves propagating at the same frequency in opposite directions have different values of k_x and k_z. Figure 1(b) shows this for the dispersion curves of the plasmons propagating in opposite directions at low wavenumbers. These are the solutions of the dispersion relation (6) yielding real values of k_z and imaginary values of k_x. The parameters used are two different electron densities $n_0^{(1)} = 10^{11}$ cm^{-2} and $n_0^{(2)} = 4 \times 10^{11}$ cm^{-2}, $\varepsilon_\mathrm{d} = 12.8$, $m = 0.067 m_0$ (corresponding to GaAs), $w = 100$ nm, and the same dc current density $J_0 = en_0^{(1),(2)} v_0^{(1),(2)} = 0.05$ A/cm. The non-reciprocal nature of plasmon propagation is pronounced for the lower electron density, where the wavenumbers of the counter-propagating plasmons at 1 THz differ by a factor of about 1.5. Hence, the decay lengths of the two plasmons also differ, as shown schematically in Fig. 1(b).

Apart from the two plasmons shown in Fig. 1(b), the channel can, at low frequencies, support two more plasmons that have higher wavenumbers and are analogous to the slow and fast space-charge waves propagating on electron beams [17]. At 1 THz, for example, the corresponding wavenumbers are 2463.8 and -1616.7 rad/μm for the channel with the dc electron density $n_0^{(2)}$. In addition, for the small value of w chosen, the dispersion relation yields infinite number of solutions with complex-valued k_z and k_x. These represent evanescent modes that decay along both the x- and z-directions. The fields in the channel are given, in general, by a superposition of all modes, low- and high-wavenumber plasmons and evanescent waves, as discussed next.

Consider an interface between the two channels with electron densities $n_0^{(1)}$ and $n_0^{(2)}$ and dc current J_0 flowing through it. A plasmon incident on the interface partially reflects and transmits, as shown schematically in Fig. 2 where the step represents the change in the dc electron density.

To solve the problem of plasmon transmission and reflection, boundary conditions at the interface $z = 0$ should be known. Our approach to the boundary conditions differed markedly from the one usually used to describe reflection of drifted plasmons [8–12]. Instead of postulating the boundary conditions at the single point $z = 0$, $x = 0$ of the junction between the channels, we consider them at the whole interface $z = 0$, $x \in [-w, w]$. Everywhere except the junction, the interface is a continuous dielectric, and the standard field boundary conditions apply

$$\begin{aligned} E_x^{(1)}|_{z=0} &= E_x^{(2)}|_{z=0} \\ H_y^{(1)}|_{z=0} &= H_y^{(2)}|_{z=0} \end{aligned} \tag{7}$$

#169158 - $15.00 USD Received 23 May 2012; revised 29 Jun 2012; accepted 2 Jul 2012; published 13 Aug 2012

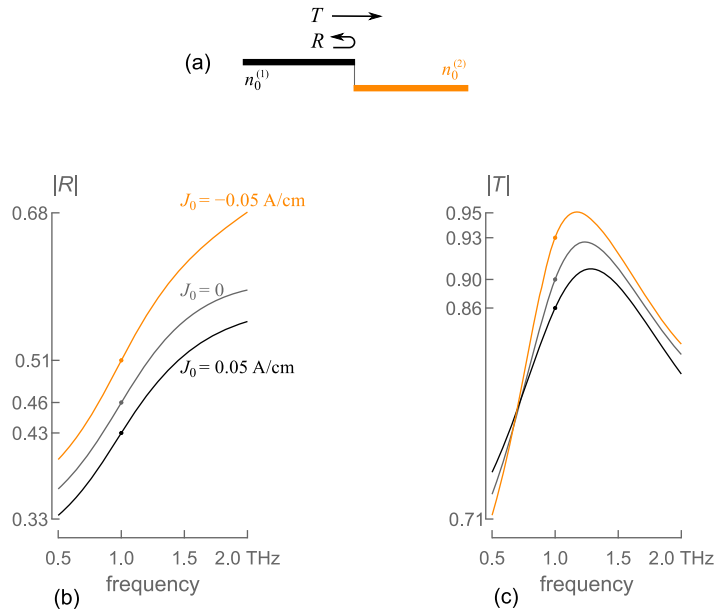

Fig. 2. Schematic presentation (a) of an interface between two different channels, where the step shows the change in the dc electron density. The presence of dc current affects the (b) reflection and (c) transmission coefficients of the plasmon incident from the channel with a larger electron density. Both coefficients can increase when the current flows away from the interface.

To solve the problem in the presence of dc current, the boundary conditions for the ac current and velocity at the junction $z = 0$, $x = 0$ should also be known. We discuss first the ac current density. Due to the symmetry of the structure, Eq. (1) gives

$$J^{(1),(2)}(z) = 2H_y^{(1),(2)}(z)|_{x=0}\,, \tag{8}$$

so that the boundary condition for the current should follow from the conditions for the magnetic field. To obtain these, we considered a cylinder of a small radius δ with the axis at the junction as shown in Fig. 3. The surface of the cylinder is in the dielectric, where the magnetic

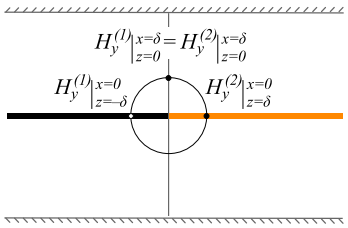

Fig. 3. To obtain the boundary conditions for the current, we surround the interface by a cylinder with a small radius δ. As the radius decreases, the difference between the magnetic fields at the cylinder surface vanishes leading to continuity of the current.

#169158 - $15.00 USD Received 23 May 2012; revised 29 Jun 2012; accepted 2 Jul 2012; published 13 Aug 2012

field is a continuous function. Hence, as the radius of the cylinder decreases, $\delta \to 0$, one gets

$$\begin{array}{l} H_y^{(1)}|_{z=-\delta}^{x=0} \to H_y^{(1)}|_{z=0}^{x=\delta} \\ H_y^{(2)}|_{z=\delta}^{x=0} \to H_y^{(2)}|_{z=0}^{x=\delta} \end{array} \tag{9}$$

and because $H_y^{(1)}|_{z=0}^{x=\delta} = H_y^{(2)}|_{z=0}^{x=\delta}$, one gets $H_y^{(1)}|_{z=-\delta}^{x=0} \to H_y^{(2)}|_{z=\delta}^{x=0}$, or, due to Eq. (9), $J^{(1)}|_{z=-\delta} \to J^{(2)}|_{z=\delta}$. As a point discontinuity of the current is implausible, the latter finally leads to

$$J^{(1)}|_{z=0} = J^{(2)}|_{z=0}\,. \tag{10}$$

Hence, the ac current density is continuous at the junction. As then follows from the continuity equation, no line charge can accumulate at the junction. The same arguments are valid for the E_x component, and hence, for the ac charge density at the interface, leading to

$$n^{(1)}|_{z=0} = n^{(2)}|_{z=0}\,. \tag{11}$$

Finally, from Eqs. (10) and (11), the boundary condition for the electron velocity is

$$v^{(2)}|_{z=0} = \frac{n_0^{(1)} v^{(1)}|_{z=0} + (v_0^{(1)} - v_0^{(2)}) n^{(1)}|_{z=0}}{n_0^{(2)}}\,. \tag{12}$$

Due to the different decay lengths of the incident, reflected, and transmitted plasmons (see Fig. 1(b)), other modes will be excited in addition to the plasmons to match the fields. Moreover, because the decay lengths of the drifting and non-drifting plasmons are different, plasmon reflection and transmission will depend on the dc current. We described the fields in the incident channel as a superposition of the incident and reflected plasmons (see Fig. 1(b)), the reflected evanescent waves, and the reflected high-wavenumber plasmons discussed above. For example, for the magnetic field, we took $H_{y1}^{(1)+} + \sum_\alpha R_\alpha H_{y\alpha}^{(1)-}$, where the superscripts + and − denote the propagation direction; the subscript α denotes the mode number (the low-wavenumber plasmons have $\alpha = 1$). The amplitude of the incident plasmon is unity, and R_α are the mode reflection coefficients. Analogously, for the transmitted magnetic field, we took $\sum_\alpha T_\alpha H_{y\alpha}^{(2)+}$, where T_α are the transmission coefficients, and the summation is for low- and high-wavenumber plasmons and the evanescent waves. The boundary conditions (7) take then the form

$$\begin{array}{l} E_{x1}^{(1)+} + \sum\limits_\alpha R_\alpha E_{x\alpha}^{(1)-} = \sum\limits_\alpha T_\alpha E_{x\alpha}^{(2)+} \\ H_{y1}^{(1)+} + \sum\limits_\alpha R_\alpha H_{y\alpha}^{(1)-} = \sum\limits_\alpha T_\alpha H_{y\alpha}^{(2)+} \end{array} \tag{13}$$

Combining Eqs. (13) with the analogous expressions for the electron velocity and current density, which follow from Eqs. (10) and (12), and using the orthogonality relation [18]

$$\int_0^w \left(E_{x\alpha}^{(1,2)} H_{y\beta}^{(1,2)} + E_{x\beta}^{(1,2)} H_{y\alpha}^{(1,2)} \right) \mathrm{d}x + \frac{m v_0^{(1,2)}}{2e} \left(J_\alpha^{(1,2)} v_\beta^{(1,2)} + J_\beta^{(1,2)} v_\alpha^{(1,2)} \right) = 0, \quad \alpha \neq \beta\,, \tag{14}$$

we were able to follow the steps of standard mode decomposition techniques [19, 20] and find numerically the values of the reflection and transmission coefficients.

As our calculations showed, the interface can amplify both the transmitted and the reflected plasmons in the presence of dc current. Figure 2 shows the reflection and transmission coefficients of the plasmon incident in the positive z-direction from the channel with the density $n_0^{(1)}$

#169158 - $15.00 USD Received 23 May 2012; revised 29 Jun 2012; accepted 2 Jul 2012; published 13 Aug 2012

upon the channel with the density $n_0^{(2)}$. When the dc current flows away from the interface (is negative), the values of the reflection and transmission coefficients can exceed those without the current. Conversely, these values can reduce for opposite dc current. Although plasmons are amplified at the interface, the effect is too weak to be used in oscillators. Indeed, a resonator is capable of oscillations only if its roundtrip gain exceeds unity, which requires high reflection coefficients. In the example of Fig. 2(b), however, the reflection coefficient increased from 0.46 to only 0.51 at 1 THz.

3. Distributed plasmonic reflectors and oscillators

To solve the problem of weak amplification at a single reflector, we combined multiple interfaces into a distributed Bragg reflector of Fig. 1(a). Optical Bragg reflectors made of dielectric layers can have high reflection coefficients due to stop bands induced by the layer periodicity. This effect was also observed in two-dimensional superlattices [21] similar to that of Fig. 1(a). In addition, our plasmonic reflectors provide distributed gain, leading to reflection coefficients larger than unity.

We analyzed the distributed reflectors by modifying the approach used in the optics of multilayers [22] as follows. Above, we obtained the transmission and reflection coefficients of plasmons incident on the interface in the positive z-direction; we now denote these as $t^{(+)}$ and $r^{(+)}$, respectively. Then, we reversed the incidence direction and obtained another pair of reflection and transmission coefficients, $t^{(-)}$ and $r^{(-)}$. If the lengths of the channels in a reflector are large enough, the evanescent waves excited at one interface do not influence the field distributions at the neighboring interfaces. As numerical calculations showed, evanescent waves in our examples can be neglected if the lengths exceed 200 nm. In addition, we ignored in the following the high-wavenumber plasmons. Because of the large wavenumber difference, scattering into these modes is ineffective, and their amplitudes are low. Under these assumptions, the four coefficients, $t_i^{(+,-)}$ and $r_i^{(+,-)}$, fully describe the i-th interface in a distributed reflector. The transmission and reflection coefficients for a reflector comprising N interfaces, $R_N^{(+,-)}$ and $T_N^{(+,-)}$, can then be found by recursive Airy summation. For example, the reflection coefficient for the plasmon incident on the reflector from the positive direction, is

$$R_N^{(+)} = R_{N-1}^{(+)} + \frac{T_{N-1}^{(+)} T_{N-1}^{(-)} r_N^{(+)} e^{-\mathrm{j}\left[k_{N-1}^{(+)} - k_{N-1}^{(-)}\right] L_{N-1}}}{1 - r_N^{(+)} R_{N-1}^{(-)} e^{-\mathrm{j}\left[k_{N-1}^{(+)} - k_{N-1}^{(-)}\right] L_{N-1}}}, \tag{15}$$

where $k_{N-1}^{(+)}$ and $k_{N-1}^{(-)}$ are the wavenumbers of the counter-propagating plasmons in the $(N-1)$-th channel that has the length L_{N-1}.

Following this approach, we analyzed a reflector consisting of seven channels with the densities $n_0^{(1)}$ and $n_0^{(2)}$, each 200 nm long, as shown schematically in Fig. 4(a). The plasmon was incident from the left (positive z-direction). In the absence of dc current, the frequency variation of the reflection and transmission coefficients has the expected Bragg-like form (see Fig. 4(b)). In a number of frequency bands, the reflection coefficient is close to unity, and the transmission coefficient is close to zero. The lack of periodicity in the curves is due to plasmon dispersion (see Fig. 1(b)).

The presence of dc current affects the transmission through and reflection from the distributed reflector (see Figs. 4(c) and (d)). Notably, the reflection coefficient exceeds unity at a number of frequencies when the current is negative (is opposite to the incidence direction), Fig. 4(d). For example, $|R^{(-)}| = 1.09$ at 1 THz for $J_0 = -0.05$ A/cm. It is, however, less than unity at the same frequencies for the positive dc current, Fig. 4(c). At 1 THz and $J_0 = 0.05$ A/cm, $|R^{(+)}| = 0.91$.

#169158 - $15.00 USD Received 23 May 2012; revised 29 Jun 2012; accepted 2 Jul 2012; published 13 Aug 2012

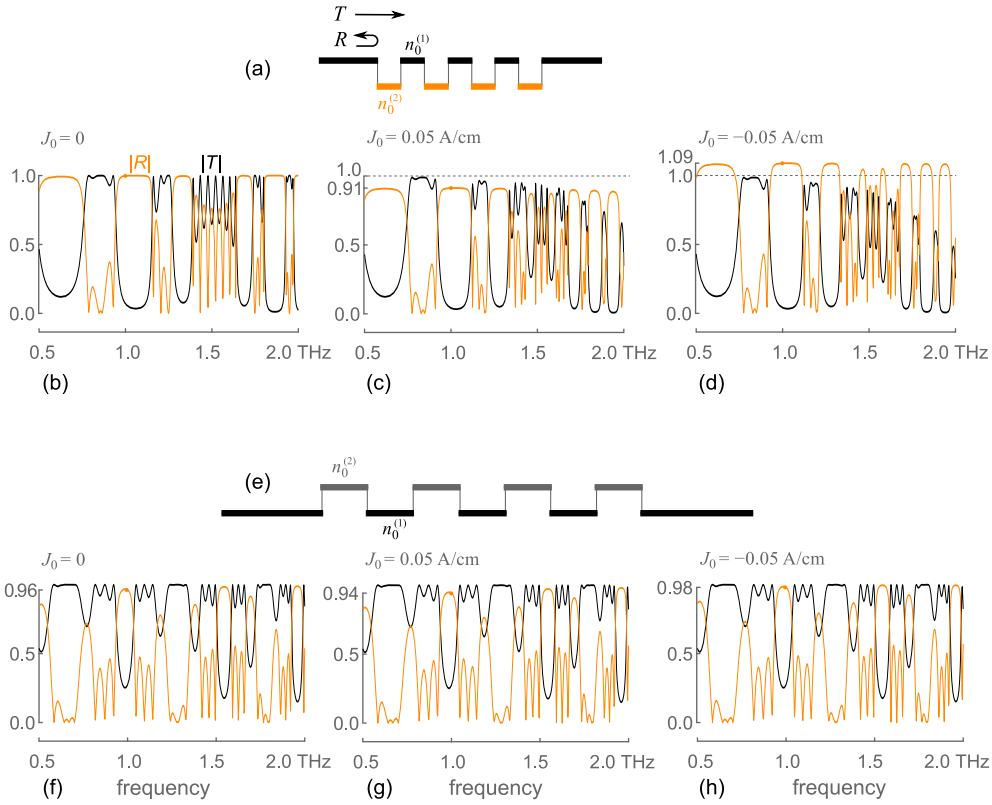

Fig. 4. The effect of the dc current depends on the structure of a distributed reflectors. In the absence of the current, (b) and (f), the plasmonic reflection coefficient can be close to unity in several frequency bands. It can increase and exceed unity for negative current densities, (d) and (h), and decrease for positive current densities, (c) and (g). The effect of the dc current is larger for the reflector (a) comprising channels with low electron density.

Because opposite currents have opposite effects on the reflection coefficient, resonators made of two identical reflectors do not oscillate. Plasmons in a resonator are incident on the reflectors from opposite directions, which is equivalent to having the reflectors at opposing currents. Amplification at one reflector is compensated by deamplification at the other, and the roundtrip gain in the resonator is the same as without the dc current. Referring to the above example, the roundtrip gain is $|G| = |R^{(-)}R^{(+)}| = 1.09 \times 0.91 \approx 1$.

To obtain a resonator with the roundtrip gain exceeding unity, we had to mitigate the reduction of the reflection coefficient at positive currents while preserving its increase at negative currents. To do so, we considered a second reflector consisting of seven channels with the electron densities $n_0^{(2)} = 4 \times 10^{11}$ cm^{-2} and $n_0^{(3)} = 10 \times 10^{11}$ cm^{-2} each 1000 nm long. It is shown schematically in Fig. 4(e) where longer lines show the increased channel lengths. The effect of the dc current on the transmission and reflection coefficients is now reduced (see Figs. 4(f)–(h)). The absolute value of the reflection coefficient at 1 THz changes from 0.96 at zero current to 0.94 at the positive and to 0.98 at the negative current.

Consider now the structurally asymmetric resonator formed by the two reflectors as shown in Fig. 5(a). For the dc current density of 0.05 A/cm, the roundtrip gain at 1 THz is equal to the product of the reflection coefficients, 1.09 and 0.94, and exceeds unity. This resonator

#169158 - $15.00 USD Received 23 May 2012; revised 29 Jun 2012; accepted 2 Jul 2012; published 13 Aug 2012

is, thus, capable of oscillations. The oscillation frequency can be intrinsically controlled by the length of the middle section in the resonator. To further prove this point, we calculated the transmission and reflection coefficients for the plasmons incident on the resonator from opposite directions. To observe oscillations at 1 THz, we chose the length of the middle section to be around 200 nm. In the absence of dc current, neither reflection nor transmission coefficient exceeds unity (Fig. 5(b)). They grow as the current increases. The oscillations occur at $J_0 = 0.029$ A/cm, when a high and narrow peak appears at 1 THz (see Fig. 5(c) and (d)).

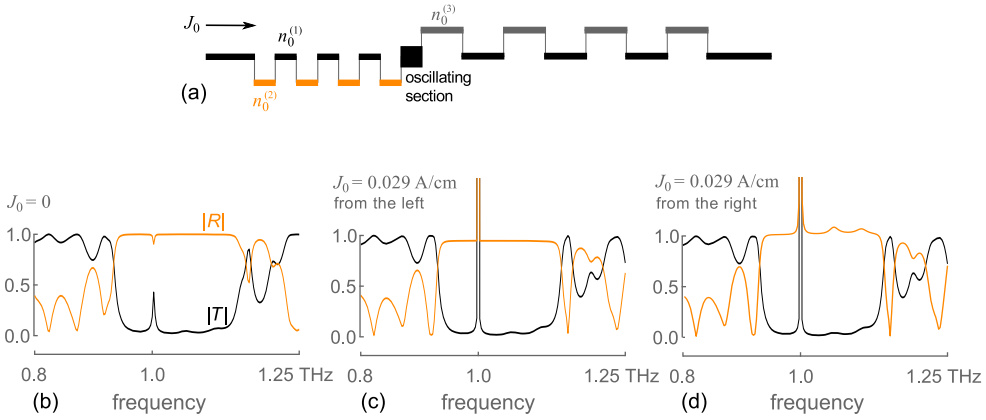

Fig. 5. Two different reflectors form an asymmetric resonator (a) whose roundtrip gain can exceed unity. The reflection and transmission coefficients of plasmons incident on the resonator do not exceed unity in the absence of the dc current (b), but oscillations occur at 1 THz when the threshold current density is reached (c) and (d). The oscillation frequency was controlled by choosing the length of the middle section.

The threshold behavior of the oscillations can be clearly seen from Fig. 6 that shows the reflection coefficient of the plasmon incident from the right against the dc current density. The circles are results of numerical calculations by the method exemplified by Eq. (15). The solid line is obtained by polynomial interpolation of the reflection coefficients of the individual interfaces and the plasmon wavenumbers of the individual channels. In each case, $|R|$ rises rapidly near the threshold current.

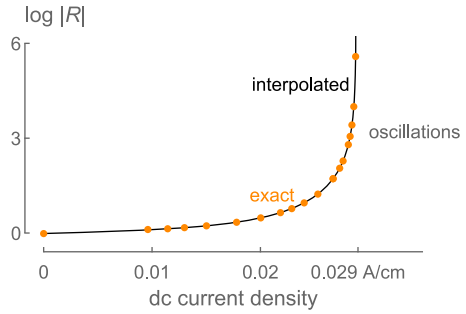

Fig. 6. A plasmonic reflection coefficient clearly shows threshold oscillation behavior. Oscillations occur at current densities exceeding 0.029 A/cm.

The presence of loss, eg. due to electron collisions, will decrease the roundtrip gain. If the loss is small, the transmission and reflection coefficients of a single reflector discussed in the

#169158 - $15.00 USD Received 23 May 2012; revised 29 Jun 2012; accepted 2 Jul 2012; published 13 Aug 2012

previous section are unlikely to be affected greatly. The loss will, however, play a role in distributed reflectors, where plasmons propagate in lossy channels. It can be accounted for in Eq. (15) by replacing the values of the propagation constants by complex numbers of the form $k' - \mathrm{j}k''$, where k'' is the attenuation constant. Assuming that the attenuation constants are equal for all channels, we studied the effect of loss for the distributed reflector of Fig. 4(a). At 1 THz, the reflection coefficients decreased linearly with small k''. The decrease of $|R|$ of 5%, from 1.09 to about 1.04, was reached for $k'' \approx 2$ rad$/\mu$m. For this value, we estimated $\omega\tau \approx 50$, where τ is the collision time. The corresponding mobilities are of the order of 10^5 cm^2/(Vs), achievable in GaAs channels at low temperatures.

4. Conclusions

We have proposed a terahertz oscillation mechanism based on distributed gain in plasmonic reflectors that comprise cascaded two-dimensional channels. The plasmonic reflection coefficient exceeds unity when plasmons are incident in the direction opposite to the dc current flow, leading to amplification. The opposite effect of deamplification occurs when the incidence direction coincides with the dc current flow. In a resonator comprising two such reflectors, plasmons propagate in both directions and, therefore, both amplification and deamplification occur. As our calculations showed, the plasmonic amplification and deamplification cancel each other if the two reflectors are identical. However, the resonators comprising two different reflectors were capable of oscillations. The threshold current density of 0.029 A/cm in our demonstrative example corresponded to the maximum drift velocity of about 2×10^6 cm/s and it could be further decreased by increasing the number of sections in the distributed reflectors. The results suggest a new way of realizing THz oscillators.

#169158 - $15.00 USD Received 23 May 2012; revised 29 Jun 2012; accepted 2 Jul 2012; published 13 Aug 2012